



SCIENTIFIC LETTER

Secondary sclerosing cholangitis: A complication after severe COVID-19 infection

Colangitis esclerosante secundaria: una complicación tras la infección severa por COVID-19

Introduction

Infection by the SARS-COV-2 coronavirus causes mainly respiratory symptoms. However, it is also known to cause systemic involvement. Liver enzyme abnormalities have been reported in over half of hospitalised patients.¹

Since the start of the pandemic, there have been several reported cases of patients developing secondary sclerosing cholangitis or post-COVID-19 cholangiopathy. This is a new condition which seems to be caused by factors already described in secondary sclerosing cholangitis in critically ill patients (SSC-CIP), but to which is also added the potential direct damage produced by SARS-COV-2 in the biliary epithelium. It is known that the virus can enter cells through the angiotensin-Converting enzyme 2 (ACE2) receptor, a receptor expressed in different cells of the human body, including cholangiocytes, so it is possible that there is a direct interaction between SARS-COV-2 and the biliary epithelium.²

The aim of this study was to analyse the development of cholangiopathy and subsequent sclerosing cholangitis in patients who required admission to the Intensive Care Unit (ICU) due to SARS-COV-2 coronavirus infection in a particular health area.

Material and methods

In this retrospective observational study, we included all patients admitted to the ICU of a health area in the Autonomous Region of Madrid from March 2020 to September 2021 with symptoms related to SARS-COV-2 infection and with positive PCR for the same. Patients with persistent changes in their liver function profile, predominantly cholestatic (understood as an increase in alkaline phosphatase [AP] >1.5 or gamma-glutamyl transferase [GGT] >3 times the upper limit of normal after transfer out of ICU) had a liver disease study performed, which included in all cases hepatotropic virus serology, hepatospecific immunity,

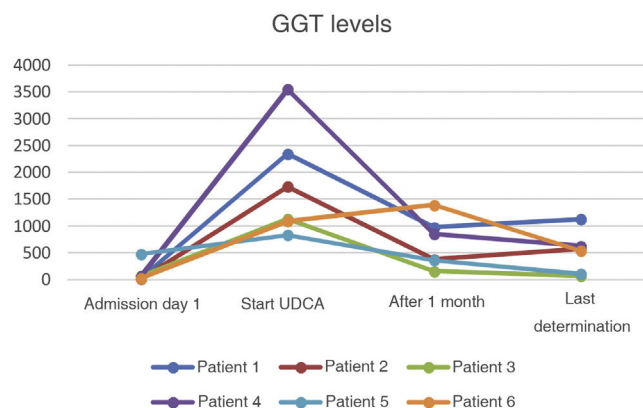


Figure 1 Changes in gamma-glutamyl transferase values over time in the different cases.

immunoglobulins, liver Doppler and nuclear magnetic resonance cholangiography.

Results

We included 334 patients admitted to ICU during the study period. Of these, six cases of post-COVID cholangiopathy (1.8%) were identified, none of whom had a previous history of liver disease. The clinical characteristics of these patients are shown in Table 1.

Four men and two women were diagnosed with a mean age of 61 ± 8.8 years: 66% with a body mass index >25; none active smokers; and five without abusive consumption of alcohol (>4 standard drink units per day [>2 in women]).

All of them (100%) developed acute respiratory distress syndrome requiring invasive mechanical ventilation, vasoactive drugs (noradrenaline, dopamine), enoxaparin and prone-supine positioning cycles (range 2–8). The mean stay in ICU was 35.5 days. At least 50% required high positive end-expiratory pressure (PEEP >10).

In all cases, intrahepatic bile duct abnormalities were identified on magnetic resonance cholangiography. All had multiple short strictures and small saccular dilations without images suggestive of lithiasis. No abnormalities were found in the extrahepatic bile duct.

All six patients were prescribed ursodeoxycholic acid at doses of 10–15 mg/kg, with a decrease in cholestasis enzymes (GGT and AP) in all cases but no simultaneous decrease in bilirubin (Bi) values (Figs. 1–3).

Table 1 Patient characteristics.

Characteristics	Patient 1	Patient 2	Patient 3	Patient 4	Patient 5	Patient 6
Age, years	63	66	60	65	44	68
Gender	Male	Female	Male	Male	Female	Male
BMI	23.9	33.9	28.4	25	40.8	22.4
Comorbidities						
<i>Smoker</i>	No	No	Former smoker	Former smoker	No	Former smoker
<i>Alcohol consumption^a</i>	No	No	Yes	No	No	No
<i>HT</i>	No	Yes	No	Yes	No	No
<i>Diabetes mellitus</i>	No	Yes	No	No	No	Yes
<i>Dyslipidaemia</i>	No	No	Yes	Yes	No	Yes
<i>Liver disease</i>	No	No	No	No	No	No
Total days hospitalised	98	37	61	81	77	79
ICU admission						
<i>Days in ICU</i>	60	19	24	46	33	31
<i>APACHE II</i>	11	10	5	20	5	16
<i>IMV</i>	Yes	Yes	Yes	Yes	Yes	Yes
<i>Maximum PEEP</i>	13	16	15	N/A	N/A	N/A
<i>No. pron-sup</i>	6	2	6	8	4	4
<i>TPN</i>	No	No	No	No	No	No
<i>Vasopressors</i>	NA ^e and DA	NA and DA	NA	NA	NA	NA
Treatment						
<i>Hydroxychloroquine</i>	Yes	No	No	No	No	No
<i>Corticosteroids</i>	Yes	Yes	Yes	Yes	Yes	Yes
<i>Tocilizumab</i>	Yes	Yes	Yes	Yes	Yes	Yes
<i>Baricitinib</i>	Yes	No	No	No	No	No
<i>Anakinra</i>	No	No	No	No	No	No
<i>Remdesivir</i>	No	No	No	No	No	No
<i>Enoxaparin</i>	Yes, anticoagulant	Yes, prophylactic	Yes, anticoagulant	Yes, anticoagulant	Yes, prophylactic	Yes, anticoagulant
<i>Antibiotics</i>	Yes	Yes	Yes	Yes	Yes	Yes
<i>Antifungals</i>	Yes	No	No	Yes	Yes	Yes
<i>Other antivirals</i>	No	No	No	Yes	No	No
Other complications						
<i>ARDS</i>	Yes	Yes	Yes	Yes	Yes	Yes
<i>PE</i>	Yes	No	Yes	No	No	Yes
<i>Acute kidney injury</i>	Yes	No	No	No	No	No
Analytical data						
<i>Admission day 1</i>						
AP (U/l)	55	80	80	65	78	50
GGT (U/l)	27	15	143	65	83	26
AST (U/l)	29	20	48	82	85	29
ALT (U/l)	17	17	32	57	52	13
Bi, total (mg/dl)	0.42	0.43	0.89	0.86	0.48	0.73
Cholesterol (mg/dl)	162	141	126	122	213	117
D-dimer	2419	200	463	397	999	945
Albumin ^b (g/dl)	4.2	4.2	3.8	3.8	3.2	3
Platelets ^b	154,000	138,000	126,000	59,000	363,000	147,000
INR	1.04	1.28	1.15	1.74	1.09	1.06
<i>Maximum value (days since onset^c)</i>						
AP (U/l)	1310 (81)	1097 (163)	248 (60)	1237 (71)	312 (74)	1650 (58)
GGT (U/l)	2594 (68)	2172 (30)	1130 (60)	3550 (71)	851 (74)	2323 (30)
AST (U/l)	1520 (55)	1048 (26)	60 (60)	250 (61)	148 (73)	500 (58)
ALT (U/l)	1000 (55)	1966 (30)	125 (60)	265 (67)	458 (59)	337 (71)
Bi, total (mg/dl)	6.21 (329)	2.82 (172)	1.45 (293)	3.24 (247)	0.77 (73)	15.03 (150)
Cholesterol (mg/dl)	875 (329)	296 (30)	217 (124)	252 (87)	231 (24)	1240 (91)
D-dimer	7418 (22)	1068 (24)	58,325 (10)	7059 (30)	3807 (16)	1470 (14)
Albumin ^b (g/dl)	2.5 (68)	2.7 (162)	2.7 (11)	2.2 (386)	2.9 (16)	2.1 (82)
Platelets ^b	37,000 (41)	76,000 (416)	94,000 (30)	90,000 (44)	200,000 (30)	145,000 (31)

Table 1 (Continued)

Characteristics	Patient 1	Patient 2	Patient 3	Patient 4	Patient 5	Patient 6
INR	1.56 (23)	2.08 (157)	1.27 (40)	1.34 (46)	1.4 (35)	1.56 (258)
<i>Last data (days since onset)^c</i>						
AP (U/l)	941 (452)	541 (416)	81 (293)	787 (394)	135 (298)	544 (158)
GGT (U/l)	1129 (452)	571 (416)	69 (293)	627 (394)	103 (298)	538 (158)
AST (U/l)	217 (452)	106 (416)	11 (293)	148 (394)	33 (298)	157 (158)
ALT (U/l)	181 (452)	82 (416)	16 (293)	75 (394)	27 (298)	136 (158)
Bi, total (mg/dl)	5.63 (452)	2.12 (416)	1.45 (293)	1.54 (394)	0.6 (298)	13.05 (158)
Cholesterol (mg/dl)	649 (452)	196 (416)	180 (293)	137 (394)	170 (298)	616 (154)
D-dimer	551 (452)	200 (282)	378 (158)	917 (69)	383 (89)	1218 (37)
Albumin (g/dl)	3.6 (452)	3.1 (416)	4.5 (293)	2.7 (394)	4.3 (298)	2.8 (158)
Platelets	261,000 (452)	76,000 (416)	123,000 (293)	95,000 (394)	301,000 (298)	235,000 (158)
INR	1.36 (452)	1.43 (416)	0.95 (293)	1.06 (394)	1.07 (147)	1.14 (158)
<i>Days since onset of symptoms-onset of cholestasis^d</i>	47	22	7	30	9	7
UDCA	Yes	Yes	Yes	Yes	Yes	Yes
MRI-cholangiogram						
<i>Extrahepatic duct</i>	Not affected	Not affected	Not affected	Not affected	Not affected	Not affected
<i>Intrahepatic duct</i>	Affected	Affected	Affected	Affected	Affected	Affected
PHT data	Yes	Yes	No	Yes	No	No
<i>Days since onset of symptoms</i>	428	421		281		
<i>Thrombocytopenia</i>	No	Yes		Yes		
<i>Hypoalbuminaemia</i>	No	Yes		Yes		
<i>Splenomegaly</i>	No	Yes		Yes		
<i>Portal vein >13 mm</i>	Yes	Yes		Yes		
<i>Varices</i>	Yes	– ^e		– ^e		
<i>Portal hypertensive gastropathy</i>	Yes	– ^e		– ^e		
<i>Decompensation</i>	No	No		Yes, ascites		
Complications after diagnosis						
<i>Death</i>	No	No	No	No	No	No
<i>Pruritus</i>	No	No	No	No	No	Yes
<i>Cholangitis</i>	No	No	No	No	No	Yes
<i>Assessed for LT</i>	Yes	No	No	No	No	No
<i>Other</i>	No	No	No	No	Cholecystectomy	Cholecystectomy

ALT: alanine aminotransferase; AP: alkaline phosphatase; ARDS: acute respiratory distress syndrome; AST: aspartate aminotransferase; Bi, total: total bilirubin; BMI: body mass index; DA: dopamine; GGT: gamma-glutamyl transferase; HT: hypertension; IMV: invasive mechanical ventilation; INR: international normalised ratio; LT: liver transplantation; MRI: magnetic resonance imaging; NA: noradrenaline; N/A: not applicable; No. pron-sup: number of prone-supine positioning cycles; PEEP: positive end-expiratory pressure; PE: pulmonary embolism; PHT: portal hypertension; TPN: total parenteral nutrition; UDCA: ursodeoxycholic acid.

^a Abusive consumption of alcohol: >4 standard drink units per day (>2 in women).

^b Minimum value.

^c Days from onset of symptoms related to SARS-COV-2 infection.

^d Onset of cholestasis: defined as >1.5 times upper limit of normal (ULN) AP or >3 times ULN GGT with or without hyperbilirubinaemia.

^e Screening upper endoscopy pending.

After a follow-up period of a median of 282 days (range 89–452), none of the patients' liver function profiles have completely returned to normal and three have developed signs of portal hypertension. In patient 2, liver stiffness was measured as 38 kPa (F4) with FibroScan® (402, Echosens) during her follow-up. None of the patients in the sample had a liver biopsy.

All six cases developed hypercholesterolaemia during admission, even the previously non-dyslipidaemic patients. Due to resistance to other lipid-lowering agents, patients 1 and 6 had to be started on treatment with alirocumab, a monoclonal antibody which binds to the PCSK9 protein, and these were the cases showing the greatest deterioration in

liver function, with bilirubin levels remaining >5 mg/dl at the last follow-up.

Once discharged, three patients had to be readmitted. Patient 4 developed a pleural empyema and his first decompensation in the form of ascites was diagnosed in this context. Patient 5 consulted with repeated pain in the right hypochondriac region, for which she underwent cholecystectomy on suspicion of biliary colic. Patient 6 was admitted for a first episode of acute cholangitis without choledocholithiasis, requiring treatment with antibiotics. None of the patients have died during follow-up. At the time of writing, one of the patients is in the process of being assessed for a liver transplant at a tertiary hospital.

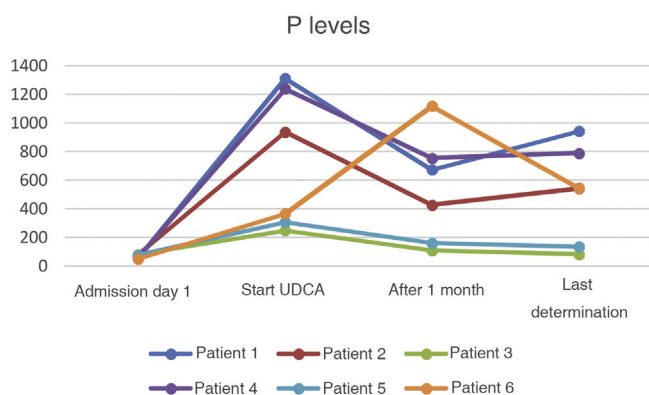


Figure 2 Changes in alkaline phosphatase values over time in the different cases.

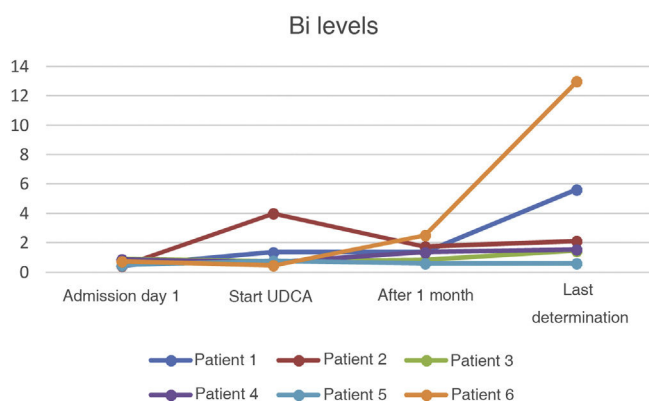


Figure 3 Changes in bilirubin values over time in the different cases.

Discussion

Secondary sclerosing cholangitis encompasses a group of chronic cholestatic diseases which affect the intra- or extrahepatic bile duct with the risk of evolving into cirrhosis. In the case of SSC-CIP, the development of advanced fibrosis seems to be particularly rapid compared to other aetiologies.³ In our sample we found progression to portal hypertension in 50% of the patients within a range of 281–428 days after the onset of COVID-19 symptoms.

It is a rare condition, rarely described in the literature, with an estimated prevalence of 0.05% of patients admitted to ICU.⁴ In our sample, post-COVID-19 cholangiopathy had an accumulated incidence of 1.8%. In other case series of post-COVID-19 cholangiopathy, the incidences calculated were 0.59%,⁵ 2.6%,¹ and 12%.⁶ Combined with our report, this suggests that there may be an added aetiological factor as well as the factors already known in the development of sclerosing cholangitis in the critically ill patient. It is likely that the direct damage of SARS-CoV-2 on cholangiocytes when interacting with receptors such as ACE2, the development of microthrombi in the biliary tree vascularisation in relation to the state of hypercoagulability that occurs during infection with COVID-19, and the magnitude of the inflammatory cascade generated in these patients are all factors to be added to the equation.⁵

However, we also have to consider that all six patients required the use of vasoactive drugs and mechanical venti-

lation with high PEEP, both of which can increase the risk of developing ischaemic cholangiopathy,⁷ and they all received potentially hepatotoxic drugs.

In our sample, all the patients were started on treatment with ursodeoxycholic acid, leading to an improvement in GGT values and, to a lesser extent, in AP during follow-up. However, there has been no parallel decrease in bilirubin values. Further studies are needed in this area, as evidence on the benefits of the drug in patients with SSC-CIP is not entirely clear. Our results could have been affected by events in the course of the disorder itself which, having only recently been described, is still not fully understood.

In any event, we believe that new prospective studies are necessary to determine the pathophysiology, prevention and treatment of this new condition, which carries the potential risk of progressive liver damage.

Funding

This study received no specific funding from public, private or non-profit organisations.

Conflicts of interest

None of the authors have any conflicts of interest.

Acknowledgements

To Dr Santos Arrontes, for his help in reviewing this manuscript.

References

- Meersseman P, Blondeel J, De Vlieger G, Van der Merwe S, Monbaliu D, Collaborators Leuven Liver Transplant program. Secondary sclerosing cholangitis: an emerging complication in critically ill COVID-19 patients. *Intensive Care Med.* 2021;47(9):1037–40, <http://dx.doi.org/10.1007/s00134-021-06445-8>.
- Klindt C, Jensen B-E, Brandenburger T, Feldt T, Killer A, chimmöller L, et al. Secondary sclerosing cholangitis as a complication of severe COVID-19: A case report and review of the literature. *Clin Case Rep.* 2021;9:e04068, <http://dx.doi.org/10.1002/ccr3.4068>.
- Peña-Pérez CA, Díaz Ponce-Medrano JA. Colangitis esclerosante secundaria en pacientes críticamente enfermos. *Cir Cir.* 2018;86:56–62, <http://dx.doi.org/10.24875/CIRU.M18000003>.
- Edwards K, Allison M, Ghuman S. Secondary sclerosing cholangitis in critically ill patients: a rare disease precipitated by severe SARS-CoV-2 infection. *BMJ Case Rep.* 2020;13:e237984, <http://dx.doi.org/10.1136/bcr-2020-237984>.
- Faruqui S, Okoli F, Olsen S, Feldman D, Kalia H, et al. Cholangiopathy after severe COVID-19: Clinical features and prognostic implications. *Am J Gastroenterol.* 2021;116:1414–25, <http://dx.doi.org/10.14309/ajg.0000000000001264>.
- Butikofer S, Lenggenhager D, Wendel Garcia P, Maggio E, Haberecker M, et al. Secondary sclerosing cholangitis as cause of persistent jaundice in patients with severe COVID-19. *Liver Int.* 2021;00:1–14.
- Martins P, Verdelho Machado M. Secondary sclerosing cholangitis in critically ill patients: An underdiagnosed entity. *GE Port J Gastroenterol.* 2020;27:103–14, <http://dx.doi.org/10.1159/000501405>.

Nazaret María Pizarro Vega*, Paz Valer Lopez-Fando,
Gema de la Poza Gómez, Belén Piqueras Alcol,
Marina Gil Santana, Paloma Ruiz Fuentes,
Marcos Alfredo Rodríguez Amado,
Fernando Bermejo San José

*Departamento de Gastroenterología, Hospital
Universitario de Fuenlabrada, Fuenlabrada, Madrid, Spain*

* Corresponding author.

E-mail address: nazaretmaria.pizarro@salud.madrid.org
(N.M. Pizarro Vega).

2444-3824/ © 2022 Elsevier España, S.L.U. All rights reserved.

Retrorectal hamartoma cyst (tailgut cyst) in a young man



Hamartoma quístico retrorectal (tailgut cyst) en paciente joven

Retrorectal cystic hamartoma also known as tailgut cyst is an uncommon congenital disease located in the presacral region-retrorectal space. It has been described in numerous anatomical locations, namely perianal, perirenal and subcutaneous involvement. Its rarity and location make it difficult to diagnose, often leading to misdiagnosis. Although it may affect individuals of all ages, this lesion occurs more frequently in middle-aged women with a 5:1 ratio.¹ It is accepted to origin from an alteration of the development of the distal end of the embryonic intestine, or tailgut. This structure reaches its largest diameter on the 35th day of gestation, and regresses by the eighth week of embryonic development. The ectoderm makes an invagination and fuses with the primitive gut to form the anus a few centimetres above its distal end, giving rise to postanal embryonic intestinal remnants with a linear tubular structure composed of 2–4 lines of cuboidal epithelium.

Due to its location, the tailgut cyst can generally be palpated by rectal examination. Whenever suspected, magnetic resonance imaging (MRI) is the most accurate non-invasive imaging technique for its diagnosis, showing a homogeneous hypodensity on T1 images and high-signal intensity on T2 images, caused by its mucinous content.² The differential diagnosis includes a wide spectrum of congenital, neoplastic, and inflammatory disorders which may be present in the presacral region. These different entities include cystic sacrococcygeal teratoma, anal gland cyst, pyogenic abscess, neurogenic cyst, and necrotic sacral chordoma.²

Although it is a benign developmental alteration, some reported cases have degenerated into a malignant adenocarcinoma originated on the epithelial layer of the tailgut cyst.³ Song et al. reported six cases that developed neuroendocrine neoplasms.⁴ The risk of malignant transformation has been reported to be about 13%, thus, complete resection of the cyst is always recommended.⁵ The risk of malignant transformation cannot be determined by any clinical, imaging or pathological characteristics. To our knowledge, there is no recognized association of the retrocecal cyst hamartoma to any other type of syndromes or malformations.

We present a case of a 26-year-old male with no relevant past medical history, who presented with sacral pain unresponsive to pharmacological therapy. An MRI study performed three years earlier in another centre showed a paracentral posterior L4–5 disc herniation. As an incidental finding, an oval retrorectal lesion measuring 31 × 22 mm was observed, which was in the presacral space anterior to the left piriformis muscle. The lesion had well-defined contours and thin walls, showing hyperintensity on T1 and T2. A second MRI was performed at our institution, showed that it had diminished its size to 25 × 20 mm. Its intensity suggested a cystic lesion with haemorrhagic or proteinaceous content. An endoscopic ultrasound fine-needle aspiration (EUS-FNA) was performed, observing a very hypoechoic lesion located in the presacral region, at 14 cm from the anal verge. The lesion had well-defined regular borders, not depending on the rectal wall, which had a normal thickness and preserved the layered echostructure (Fig. 1A). No pathologic lymph nodes were identified in the perirectal fat. A FNA was performed using a 22 G needle, obtaining purulent material for cytological diagnosis. The patient had fever and pain after the procedure, which resolved with systemic antibiotics. Cytologic analysis revealed the presence of few isolated cylindrical ciliated epithelial cells without atypia, in a background of amorphous-proteinaceous material and occasional groups of transitional-like epithelial cells (Fig. 1B, C). Cytological diagnosis was compatible with a hamartoma-tailgut cyst. Surgical resection was considered due to patient's symptoms, with a monoblock lateral dissection of the mesorectum including the presacral fascia. The post-operative course was uneventful. A fresh intact nodular lesion measuring 30 × 18 × 8 mm was received at the Pathology Department, and the entire surface was painted with black Indian ink. Gross sectioning revealed a cystic lesion with a 2 mm thick wall with yellowish areas of medium consistency, lined by a thin and smooth surface containing a brownish fluid (Fig. 1D). Histologic examination revealed a cystic lesion lined by non-dysplastic ciliated columnar pseudostratified epithelium containing mucinous cells and few lymphocytes. In some areas the epithelium showed a transitional appearance (Fig. 1E and F). The rest of the wall was composed by smooth muscle with ectasic vessels, and areas of chronic lymphohistiocytic and xanthomatous inflammation, corresponding to the FNA trajectory. The final pathological diagnosis was of retrorectal hamartoma (tailgut cyst) lined by ciliated-cylindric epithelium with mucin production and no dysplasia.